Breast Tissue Screening with Microwave Time-Domain Radar: Initial Clinical Trials

Emily Porter, Adam Santorelli, Mark Coates and Milica Popović
Electrical and Computer Engineering
McGill University
Montreal, Quebec, Canada
{emily.porter, adam.santorelli}@mail.mcgill.ca, {mark.coates, milica.popovich}@mcgill.ca

***Abstract*—In this work, we present early results from a clinical trial of our time-domain microwave breast cancer screening system. The goal of the trial is to verify use of the system for a breast monitoring application. We follow four (healthy) patient volunteers and perform regular breast scans on them over a time period of eight months. We then compare the collected data and the reconstructed breast images from the scans. We show small variation in the signals collected from individual patients over time but also consistency in the corresponding images. Our results suggest that our system successfully avoids false positives over longer screening periods. The next step in our investigations is to determine if visible differences arise if malign tissue is present.**

I. Introduction

Microwave techniques for breast cancer screening have been heavily researched in recent years. Unlike the standard X-ray mammography, these offer breast scans that do not use ionizing radiation, do not require breast compression, and that can be implemented with lower cost [1], [2]. Microwave tomography aims to reconstruct a complete dielectric profile of the tissues within the breast. Microwave radar, on the other hand, is used to construct a map of electromagnetic scatterers. The two approaches have been researched with both frequency-domain (using a network analyzer) and time-domain measurements (using a pulse generator and oscilloscope). Several have even made it to the clinical trial stage [3] – [6].

In our work, we use time-domain radar as the basis for a breast cancer screening system. Our system contains a 16-element multistatic array that operates in the 2 – 4 GHz range. This frequency band represents a trade-off between the high penetration depths possible at low frequencies (due to lower losses in the tissues) and the higher resolution (but worse loss) at high frequencies. Time-domain measurements are potentially more cost-effective than frequency-domain measurements and allow for faster scan times; however, they come with a trade-off in the signal-to-noise ratio [2].

In [7], we presented very early results from our clinical trial. Here, we provide an update on the use of our system for a monitoring application. In particular, we conducted a clinical trial that followed several patients over an eight-month period. During this interval, we perform regular monthly breast scans on them, allowing us to compare the results over time. This work presents a comparison of both the collected signal data and the processed, reconstructed images.

II. System and Methods Overview

This section describes the system setup and operation, along with a detailed description of the antenna array and radome that holds it in place. We also discuss the clinical trial and present an overview of the patients that were followed.

A. Breast Screening System Description

The system operates in the time-domain. The signal is generated by a generic pulse generator, and is then shaped to focus the content over the 2 – 4 GHz frequency range. We amplify the pulse before sending it into a 16 × 2 switching network that selects each of the 16 antennas for transmitting or receiving. The network cycles through each transmit-receive antenna-pair combination in turn, until each transmitter has sent a pulse to each receiver, for a total of 240 signals. The signal propagates through the breast and is recorded by a sampling oscilloscope that is USB-controlled by a computer. Each signal is 1024 samples long and is recorded at a time-equivalent sampling rate of 40 GSa/s. A complete system description can be found in [8].

B. Radome and Antenna Array

The antenna array contains 16 Traveling Wave Tapered and Loaded Transmission Line Antennas (TWTLTLAs, [9]). The antennas are designed for bio-sensing applications in the microwave frequency range, and are optimized to operate in close proximity with breast tissues. As the antennas have end-fire radiation, we embed them into a hemi-spherical radome for ease of interaction with the human breast.

The radome is a low-loss dielectric with relative permittivity matched to that of both the antenna substrate and the average breast adipose tissue properties. It houses the 16 antennas along its exterior surface, and the breast is placed inside the radome. We note that for clinical trials, ultrasound gel is used to fill any air gaps between the irregularly shaped breast and the radome walls.

A schematic of the radome is shown in Fig. 1 with antenna locations in the array marked. Each of the antennas is labeled Ax, where x = 1:16. A 3-D model of the radome and antenna array is also shown for ease in visualization of the antenna positions.

978-1-4799-3678-6/14/$31.00 ©2014 IEEE

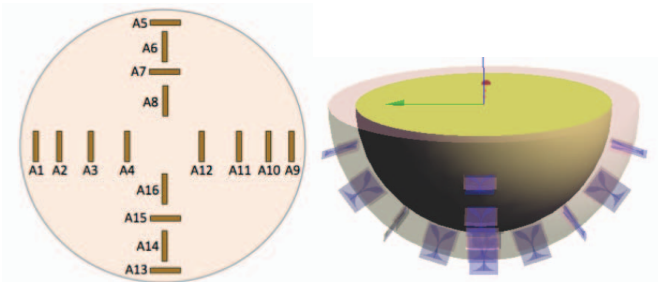

Fig. 1. Schematic layout of the antenna array on the exterior of a hemispherical radome (left), and a 3-D diagram of the same (right). The 16 antennas are labelled from A1 to A16.

C. *Clinical Trial Decription*

As is typical with early-stage clinical trials, volunteers are used to study the system behavior before it can be applied to those who are ill. We monitor four healthy volunteers over a period of six to eight months, with each woman having five to six breast scans over this period.

A summary of patient data is provided in Table I. The four volunteers are labeled Patient A, B, C, and D. For example, Patient A has had six breast scans taken over a six-month period. We denote the scans as "Scan 1", "Scan 2", ... , "Scan T", where T is equal to the total number of scans for the patient in question.

TABLE I. SUMMARY OF PATIENT DATA AND TRIAL PARTICIPATION.

Patient	Age	Cup Size	Number of Visits	Duration (months)
A	45	C	6	6
B	23	B	6	6
C	24	C	5	8
D	44	C	5	7

III. RESULTS AND DISCUSSION

We first examine a sampling of the collected signals. In Fig. 2, we plot received signals for select antenna pairs for Patient C (right breast) and Patient B (left breast). In particular, we show the signal corresponding to antenna pair A9A10 (A9 transmits, A10 receives) for all five scans of Patient C; similarly for A4A12. In this scenario, A9A10 is a recording of a reflection scenario, i.e., the antennas are located on the same side of the radome; A4A12 is a transmission scenario with the antennas located across the breast from each other. We also show the data from antenna pairs A1A2 (reflection) and A2A10 (transmission) for the six breast scans of Patient B.

From Fig. 2, it is seen that the signal shapes are consistent over all of the monthly scans for both Patients B and C. The amplitudes vary between scans; however, only late-time variations are indicative of changes in the breast tissues. This is because early-time signals represent the waves that have

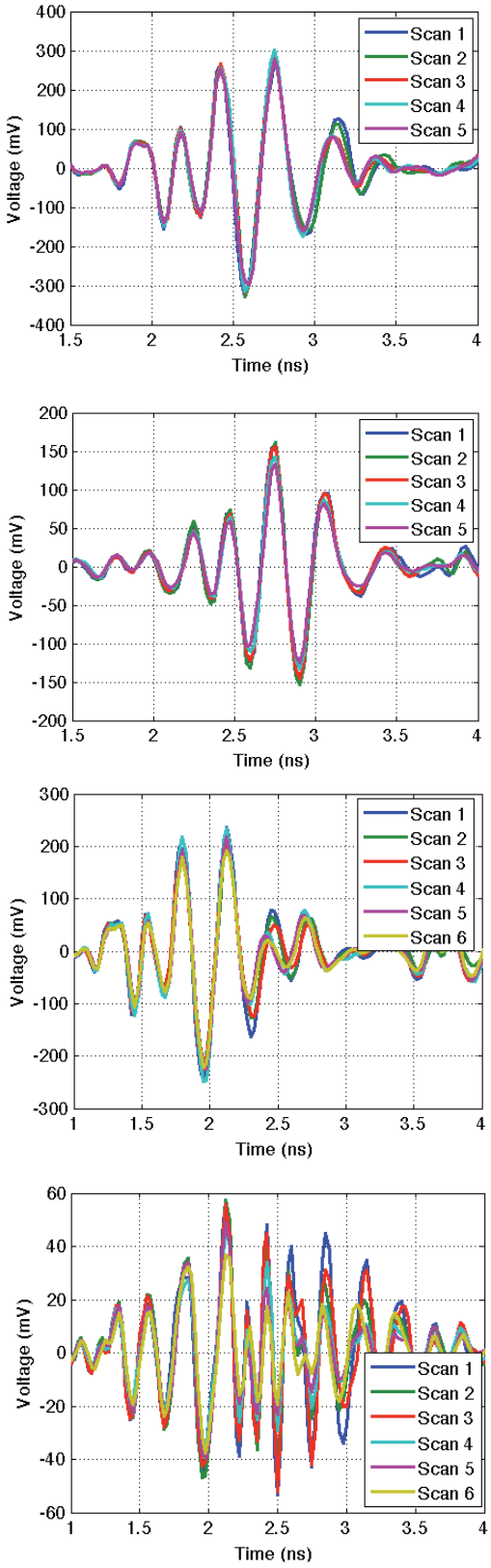

Fig. 2. Signal plots for selected antenna pairs over all monthly scans. From top to bottom: Patient C, right breast, antenna pair A9A10, antenna pair A4A12; Patient B, left breast, antenna pair A1A2, antenna pair A2A10.

travelled directly between the antennas, and not through the breast tissue. Discrepancies in early-time signals can be removed with calibration. If the variations due to the presence of malign tissue are of a similar magnitude as we have observed in our experiments with breast phantoms [10], then the variations seen here in the late-time signals are small by comparison. We note that for Patient C the scan signals vary only negligibly over the 8-month time frame, while the signals for Patient B provide an example of when the data collected does vary visibly over time. Many factors could be the source of this variation. We here note a particular factor: Patient B has a smaller cup size, resulting in a larger volume of ultrasound gel used to fill the air gaps. Changes in the distribution of the gel relative to the breast and its thickness from one scanning trial to the next can affect the consistency of the recorded signals.

Next, we examine images reconstructed from the patient breast scans. Images are generated using the Delay-Multiply-and-Sum algorithm [11]. In the images, red represents regions of high electromagnetic scattering and blue represents areas of little or no scattering. Fig. 3 shows a single 2-D slice of the image generated from Patient C (right breast) scans over five visits. Similarly, Fig. 4 shows another slice from each of the five scans of Patient D. From both figures, we see that the images are consistent over the duration from the first to the last scan, with only slight changes visible.

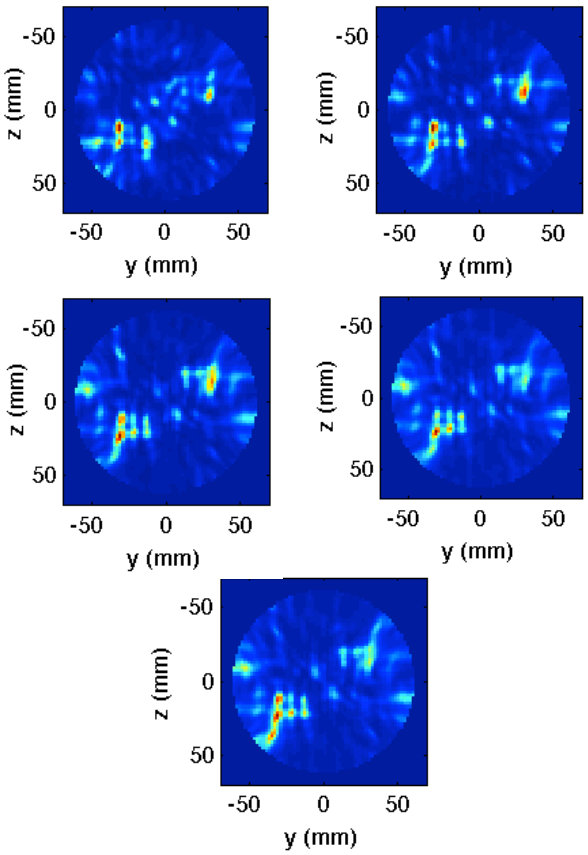

Fig. 3. Image slices from the five monthly scans of Patient C (right breast). From left to right, top row: Scan 1 and Scan 2; second row: Scan 3 and Scan 4; bottom row: Scan 5.

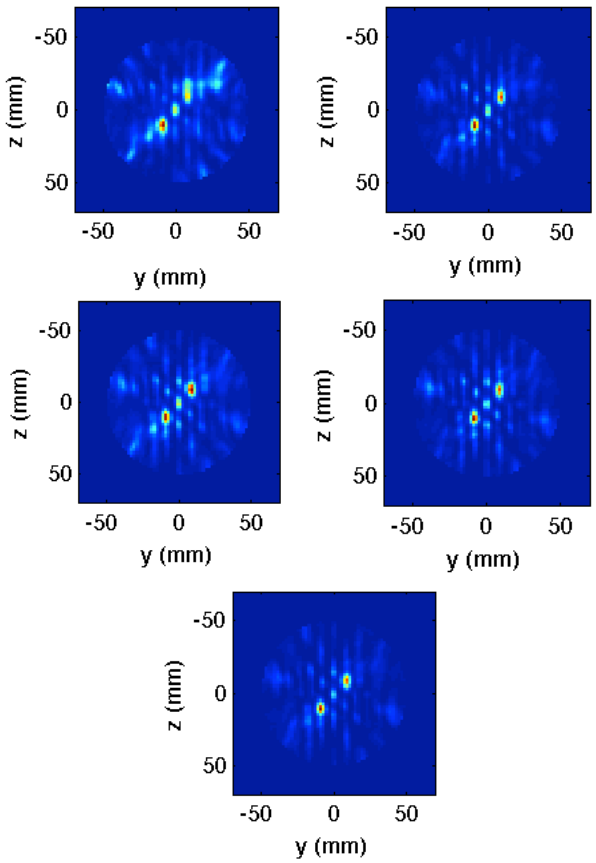

Fig. 4. Image slices from the five monthly scans of Patient D (right breast). From left to right, top row: Scan 1 and Scan 2; second row: Scan 3 and Scan 4; bottom row: Scan 5.

Finally, in Table II, we present a summary comparing the monitoring over time for each patient (both breasts). We show the peak difference, in decibels (dB), between images generated from various scans for each patient. This value is calculated by subtracting the pixel intensities from corresponding slices of different scan instances to obtain a difference image; the peak of the difference image is then determined relative to the peak of the original two images. In particular, we show the peak difference between Scans 2 and 1, and between Scans 5 and 1 (for Patients C and D) or Scans 6 and 1 (for Patients A and B). In this manner, we can observe the similarity of the successive scans (Scans 2 and 1), and that of the temporally most distant scans (Scans T and 1).

From Table II, we see the successive images are often more similar (have a lower peak difference) than scans that are taken a long time apart from each other. We also note that the difference between images is always less than -11.9 dB relative to the original image. These values indicate that differences in images not visible by the eye can be picked up through quantitative analysis. Methods to identify differences between scans, through pixel-to-pixel comparison or image structure comparison, may be applied in the future.

TABLE II. SUMMARY OF DIFFERENCES (IN DB) IN BREAST SCANS OVER THE MONITORING PERIOD FOR ALL PATIENTS.

Patient	Breast	Scan 2 – Scan 1	Scan T – Scan 1
A	***Left***	-13.2	-13.0
	Right	-12.9	-14.1
B	***Left***	-18.0	-13.9
	Right	-17.6	-16.1
C	***Left***	-15.4	-12.8
	Right	-17.0	-11.9
D	***Left***	-15.9	-14.2
	Right	-13.2	-13.5

IV. CONCLUSION

In this work we have demonstrated the application of our time-domain microwave breast cancer monitoring system with a clinical trial on human volunteers. We tracked four patients over a time frame covering six to eight months; and each patient had at least five breast scans during this period. We have shown that there is some variation in the collected signals over the trial duration; however, the reconstructed images are visually consistent.

Further research remains to be done before we can truly verify the use of our system for a breast cancer detection application. More specifically, investigations are pending on how much of a change in the images can be expected over time due to regular, healthy tissue changes, as compared to how much change could be expected for the case of undesired tissue growth, e.g. a tumor or a cyst.

ACKNOWLEDGEMENT

This work was supported by the Natural Sciences and Engineering Research Council of Canada (NSERC), Le Fonds de recherche du Québec - Nature et technologies (FQRNT), and Partenariat de recherche orientée en microélectronique, photonique et télécommunications (PROMPT). The authors are grateful to the McGill University Photonics Systems Group for allowing us access to their experimental resources.

REFERENCES

[1] E. Fear, "Microwave imaging of the breast," *Technology in Cancer Research & Treatment*, Vol. 4, No. 1, pp.69–82, Feb. 2005.

[2] X. Zeng, A. Fhager, P. Linner, M. Persson, and H. Zirath, "Experimental investigation of the accuracy of an ultrawideband time-domain microwave-tomographic system," *IEEE Trans. Instrum. Meas.*, vol. 60, no. 12, pp. 3939–3949, Dec. 2011.

[3] T. Grzegorczyk, P. M. Meaney, P. A. Kaufman, R. M. diFlorio-Alexander, and K. D. Paulsen, "Fast 3-D tomographic microwave imaging for breast cancer detection," *IEEE Trans. Med. Imag.*, vol. 31, no. 8, pp. 1584–1592, Aug. 2012.

[4] J. Bourqui, J. M. Sill, and E. C. Fear, "A prototype system for measuring microwave frequency reflections from the nreast," *International Journal of Biomedical Imaging*, vol. 2012, pp. 1–12, Article ID 851234, 2012.

[5] H. Jiang, C. Li, D. Pearlstone, and L. Fajardo, "Ultrasound-guided microwave imaging of breast cancer: Tissue phantom and pilot clinical experiments," *Med. Phys.*, vol. 32, no. 8, pp. 2528–2535, Aug. 2005.

[6] M. Klemm, I. J. Craddock, J. A. Leendertz, A. Preece D. R. Gibbins, M. Shere and R. Benjamin, "Clinical trials of a UWB imaging radar for breast cancer," in *Proc. Antennas and Propagation (EuCAP), 2010 4th European Conference on*, pp. 1–4, Barcelona, Spain, Apr. 12–16, 2010.

[7] E. Porter, A. Santorelli and M. Popović, "Breast monitoring via time-domain microwave radar: early clinical trial study," in *Proc. 36th Annual International Conference of the IEEE Engineering in Medicine and Biology Society (EMBC)*, Chicago, Illinois, U.S.A., Aug. 26–30, 2014, in press.

[8] E. Porter, E. Kirshin, A. Santorelli, M. Coates, and M. Popović, "Time-domain multistatic radar system for microwave breast screening," *IEEE Antennas Wireless Propag. Lett.*, vol. 12, pp. 229–232, 2013.

[9] H. Kanj, and M. Popović, "A novel ultra-compact broadband antenna for microwave breast tumor detection," *Prog. Electromagn. Res.,* vol. 86, pp. 169–198, 2008.

[10] A. Santorelli, M. Chudzik, E. Kirshin, E. Porter, A. Lujambio, I. Arnedo, M. Popović, and J. Schwartz, "Experimental Demonstration of Pulse Shaping for Time-Domain Microwave Breast Imaging," *Prog. Electromagn. Res.*, vol. 133, pp. 309 – 329, 2013.

[11] H. B. Lim, N. T. T. Nhung, E. P. Li, and N. D. Thang, "Confocal microwave imaging for breast cancer detection: Delay-multiply-and-sum image reconstruction algorithm," *IEEE Trans. Biomed. Eng.*, vol. 55, no. 6, pp. 1697–1704, Jun. 2008.